doi:10.1016/j.jmb.2007.07.009 J. Mol. Biol. (2007) 372, 708–722

JMB

Available online at www.sciencedirect.com

ScienceDirect

ELSEVIER

Structural Characterization of the Intrinsically Unfolded Protein β-Synuclein, a Natural Negative Regulator of α-Synuclein Aggregation

Carlos W. Bertoncini[1,2], Rodolfo M. Rasia[1], Gonzalo R. Lamberto[3] Andres Binolfi[3], Markus Zweckstetter[2,4], Christian Griesinger[2] and Claudio O. Fernandez[2,3,*]

[1]*Department of Molecular Biology, Max Planck Institute for Biophysical Chemistry Am Fassberg 11, D-37077 Göttingen, Germany*

[2]*Department of NMR-based Structural Biology Max Planck Institute for Biophysical Chemistry Am Fassberg 11, D-37077 Göttingen, Germany*

[3]*Instituto de Biología Molecular y Celular de Rosario Consejo Nacional de Investigaciones Científicas y Técnicas, Universidad Nacional de Rosario, Suipacha 531 S2002LRK, Rosario, Argentina*

[4]*DFG Center for the Molecular Physiology of the Brain D-37077, Göttingen, Germany*

**Corresponding author*

The synuclein family of intrinsically unfolded proteins is composed of three highly homologous members, α-synuclein (αS), β-synuclein (βS) and γ-synuclein (γS), which are linked to neurodegenerative disorders and cancer. αS has been studied intensively after its identification as the major protein component of amyloid-like deposits in Parkinson's disease and dementia with Lewy bodies. βS, on the other hand, was found to act as a potent inhibitor of αS amyloid formation, and it is proposed as a natural regulator of its neurotoxicity. It is then of particular interest to elucidate the structural and dynamic features of the soluble state of βS as a first step to understand the molecular basis of its anti-amyloidogenic effect on αS. We present here the characterization of natively unstructured βS by high resolution heteronuclear NMR techniques. A combination of pulse-field gradient, three-dimensional heteronuclear correlation, residual dipolar couplings, paramagnetic relaxation enhancement and backbone relaxation experiments were employed to characterize the ensemble of conformations populated by the protein. The results indicate that βS adopts extended conformations in its native state, characterized by the lack of the long-range contacts as previously reported for αS. Despite the lack of defined secondary structure, we found evidence for transient polyproline II conformations clustered at the C-terminal region. The structuring of the backbone at the C terminus is locally encoded, stabilized by the presence of eight proline residues embedded in a polypeptide stretch rich in hydrophilic and negatively charged amino acids. The structural and functional implications of these findings are analyzed *via* a thorough comparison with its neurotoxic homolog αS.

Keywords: NMR; amyloid; protein aggregation; unfolded state; polyproline II

Present addresses: C. W. Bertoncini, Department of Chemistry, University of Cambridge, Cambridge, UK; R. M. Rasia, Institut de Biologie Structurale Jean-Pierre Ebel, Grenoble, France; C. O. Fernandez, Instituto de Biología Molecular y Celular de Rosario, Consejo Nacional de Investigaciones Científicas y Técnicas, Universidad Nacional de Rosario, Suipacha 531, S2002LRK, Rosario, Argentina.

Abbreviations used: S, synuclein; PFG, pulse-field gradient; RDC, residual dipolar coupling; HSQC, heteronuclear single-quantum coherence; NOE, nuclear Overhauser enhancement; ROA, Raman optical activity; PRE, paramagnetic relaxation enhancement; DLB, dementia with Lewy bodies; MTSL, (1-oxy-2,2,5,5-tetramethyl-D-pyrroline-3-methyl)-methanethiosulfonate.

E-mail addresses of the corresponding author: cfernan@gwdg.de; fernandez@ibr.gov.ar

Introduction

Intrinsically unfolded proteins have challenged the paradigm of the structure–function relationships in current biology, since they are now recognized to play essential roles in transcription, translation and signal transduction pathways.[1] The absence of defined structure allows disordered regions of proteins to attain functional plasticity in physiological states of cells but also represents an easy target for misfolding, leading often to disease conditions.[2] Failure at the chaperone or proteasomal level diminishes the ability of the cell to clear misfolded proteins which generally coalesce into toxic soluble oligomers or insoluble amyloid-like fibrils, hallmarks of this type of pathologies.[3] Indeed, neurodegenerative disorders such as Alzheimer's or Parkinson's disease are often linked to partially or completely unfolded states of certain polypeptides that are highly aggregation-prone.[4] Hence, a tight regulation of both the abundance and function of unfolded proteins is required to circumvent harmful consequences.

An example of the unfolding–misfolding dichotomy is the Synuclein family, a closely related group of brain-enriched proteins (αS, βS and γS) that has been implicated in neurodegenerative disorders and cancer.[5] αS and βS co-localize in pre-synaptic nerve terminals, close to synaptic vesicles, while γS appears to be axonal and cytosolic.[6] Their physiological roles are poorly understood, though αS is suggested to be involved in SNARE vesicle recycling.[7] However, in pathological conditions such as Parkinson's disease (PD) or dementia with Lewy bodies (DLB), it is well known that αS adopts β-sheet-rich conformations that promote neurotoxicity, reflected in protein oligomerization and amyloid-like fibrillation.[8,9] Interestingly, βS lacks the central hydrophobic cluster in its sequence (Figure 1(a)) and has a protective role on these events *in vitro* and *in vivo*, suggesting that the protein might be a natural negative regulator of the amyloid formation of αS.[10–14] These results raise the possibility that interactions among closely homologous molecules in the same family of proteins might regulate the state of aggregation in proteins exhibiting amyloidogenic properties. Thus, the knowledge of the structural and dynamic features of βS represents the first step to the study of the molecular mechanism through which βS exerts its anti-amyloidogenic effect on αS.

High-resolution structural characterization of poorly structured proteins is a difficult task as they cannot be studied by means of crystallography. Recently, with the development of higher magnetic fields and computing methods, NMR spectroscopy became a powerful tool to elucidate the structural and dynamic features of unfolded states of proteins.[15] Indeed, by using NMR spectroscopy we and others have recently shown that in its native state αS adopts an ensemble of conformations with no significant secondary structure, although long-range interactions play an essential role to stabilize an aggregation auto-inhibited global protein architecture.[16–18] A similar study on the Parkinsonism-linked mutants of αS showed that the destabilization of specific tertiary interactions essential for the native state of αS correlates with a higher tendency to oligomerize.[19] By contrast, no high-resolution spectroscopic studies have been performed on the native state of its homologue βS; an unexplored area that needs to be investigated to assess the hierarchy of tertiary interactions in αS oligomerization and to identify the structural determinants that may reverse its aggregation.

We report here the structural characterization of the native state of βS by means of high-resolution

(a)

```
αS   1 MDVFMKGLSKAKEGVVAAAEKTKQGVAEAAGKTKEGVLYVGSKTKEGVVH  50
βS   1 MDVFMKGLSMAKEGVVAAAEKTKQGVTEAAEKTKEGVLYVGSKTREGVVQ  50

αS  51 GVATVAEKTKEQVTNVGGAVVTGVTAVAQKTVEGAGSIAAATGFVKKDQL 100
βS  51 GVASVAEKTKEQASHLGGAVFSG----------AGNIAAATGLVKREEF  89

αS 101 GKNE-----EGAPQEGILEDMPVDPDNEAYEMPSEEGYQDYEPEA 140
βS  90 PTDLKPEEVAQEAAEEPLIEPLMEPEGESYEDPPQEEYQEYEPEA 134
```

(b)

	αS		βS	
pH 6.5 + 100 mM NaCl	+	+	+	+
Urea 8 M	-	+	-	+
R_H (Å)	31.9	35.0	32.4	35.4
R_H expected for length (Å)	19.9	37.0	19.7	36.0

(c)

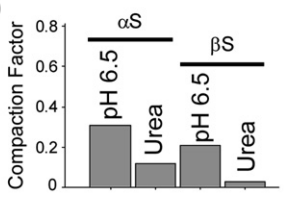

Figure 1. General characteristics of the ensemble of conformations populated by αS and βS. (a) Alignment of αS and βS amino acid sequence, displaying the absence of the central hydrophobic NAC region in βS and a shorter C terminus in αS. Shaded in grey are amino acids that differ between both proteins. (b) Comparison of hydrodynamic properties of αS and βS. Measurement of hydrodynamic radii (R_H) by PFG-NMR for αS and βS under different solution conditions. The expected R_H values are calculated based on empirical determinations on native and unfolded proteins.[20] (c) Plot of compaction factors derived from measurements in (b) according to Wilkins *et al.*[20]

NMR spectroscopic techniques. Triple resonance experiments allowed us to assign the backbone resonances of the protein in its soluble state and to evaluate its secondary structure propensities. NMR paramagnetic relaxation enhancement by nitroxide spin labels and measurement of hydrodynamic properties by pulse-field gradient (PFG) NMR indicated that βS, opposite to αS, populates more extended conformations in its native state. Regions of the C terminus exhibiting particularly high residual dipolar couplings were coincident with the population of polyprolyne II backbone conformations. In contrast to αS, backbone structuring at the C terminus of βS is mainly determined by local interactions. At the light of the distinctive structural preferences exhibited by members of the synuclein family, potentially relevant functional and biological implications are discussed.

Results and Discussion

βS populates extended conformations in solution

The effective hydrodynamic radius of βS was determined using PFG NMR techniques with the aim of obtaining an initial characterization of the ensemble of conformations populated by the protein. The measured values of the hydrodynamic radius for βS in its native state (32.4 Å) and in the presence of 8 M urea (35.4 Å) are both significantly shifted toward the value empirically calculated for a highly denatured state (36.0 Å) (Figure 1(b)). In order to estimate the degree of unfolding of the protein scaffold we calculated the compaction factor (C_f) of the ensemble (Figure 1(c)), which relates the measured R_H with empirical estimations of the minimum and maximum values expected for the length of the polypeptide chain.[20] Compared with the parameters measured for its homologue αS (C_f=0.30), the compaction factor obtained for βS in its native state (C_f=0.20) indicates that the protein might adopt an ensemble of more extended conformations in solution, as suggested by small angle scattering measurements.[11] From the ratio between the hydrodynamic dimensions measured by PFG NMR and the values of the radius of gyration (R_G) reported using small angle scattering techniques[11] a value (R_G/R_H) of 1.50 is calculated for βS, in agreement with the value predicted for a random coil polypeptide by Tanford (R_G/R_H=1.51).[21,22] Furthermore, from the hydrodynamic radius determined in 8 M urea a set of complete unfolded conformations are predicted for βS (C_f=0.04), whereas a slightly collapsed arrangement is suggested for αS (C_f=0.12). These results likely reflect the decreased persistence of the residual long-range interactions in αS, as determined by paramagnetic relaxation enhancement measurements in 8 M urea,[16] and indicate the absence of such structural features in βS.

NMR backbone assignment of βS

To understand the basis of these differences we aimed to determine the backbone structural propensities and dynamics present in βS by using heteronuclear NMR spectroscopy. The ^{1}H-^{15}N heteronuclear single-quantum coherence (HSQC) spectrum of uniformly ^{15}N-labeled βS recorded at 15 °C and pH 6.5 is shown in Figure 2. The resonances are well resolved and sharp, with a limited dispersion of chemical shifts, reflecting the unfolded nature and high degree of backbone mobility. Resonance assignment in natively unfolded proteins by the standard triple resonance experiments[23] is severely hampered because of the high degeneracy of the amide and carbon chemical shifts. In proteins from the synuclein's family, further obstacles arise from the presence of several imperfect repeats (KTKEGV) at the N-terminal domain.[24] In order to obtain complete amide ^{1}H, ^{15}N, and ^{13}C assignments in βS we performed HNN and HN(C)N experiments, that exploit the good dispersion of ^{15}N chemical shifts along two of the three dimensions and provide many checkpoints around Gly and Pro residues down the sequential walk.[25] Consequently, 98% of the chemical shifts corresponding to ^{1}H, ^{15}N, $^{13}C^{\alpha}$, $^{13}C^{\beta}$ and $^{13}C'$atoms from the backbone were successfully assigned to specific residues in the primary sequence of βS (Supplementary Data, Table 1). All the amide cross-peaks in the ^{1}H-^{15}N HSQC spectrum displayed similar intensity ratios and no evidences for the occurrence of an intermediate conformational exchange process were observed under these conditions of neutral pH and low temperature, in agreement with the data reported for αS at 10 °C.[26]

NMR reveals polyproline II propensities in βS

NMR chemical shifts, in particular those of H^{α}, C^{α}, and C′ are very sensitive probes of secondary structure in proteins.[27] Deviations of observed chemical shifts from the random coil values (secondary shifts, Δδ) are indicators of secondary structures propensities in unstructured polypeptides, providing useful information on the local degree of structure that is preferentially sampled by the backbone of such highly dynamic systems.[15] As observed in Figure 3, significant deviations in chemical shifts occur for backbone regions in βS. Slightly negative deviations were found for almost all H^{α} atoms, suggesting that backbone conformations with residual helical content are sampled (Figure 3(a)). Positive deviations in C^{α} and C′ shifts, also indicative of α-helical propensities were predominantly located at the N terminus of the protein, where the regions between amino acid residues 20–35 and 55–65 showed the strongest propensity to adopt such conformations (Figure 3(b) and (c) and Supplementary Data, Figure S1A).[28] Instead, negative deviations from C^{α} and C′ random coil shifts were predominant for the C terminus of βS, indicating some tendency to populate the β-space of the Ramachandran map, which includes both extended β conformations and poly-

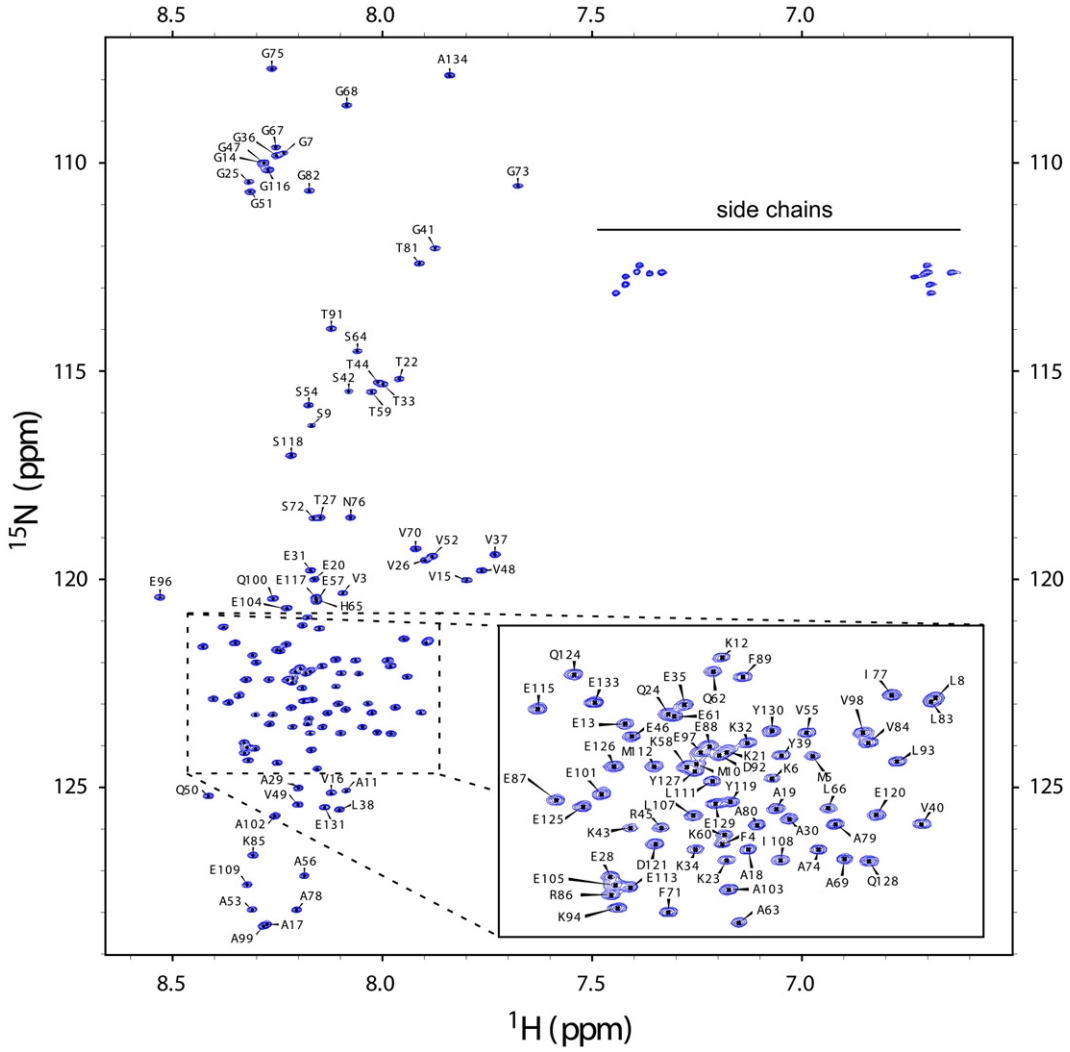

Figure 2. ^{1}H-^{15}N HSQC spectrum of βS. Assigned ^{1}H-^{15}N HSQC spectrum of βS at pH 6.5 and 100 mM NaCl, in which 124 out of 126 non-proline residues are observed.

proline II structures (Figure 3(b) and (c) and Supplementary Data, Figure S1A). The C^{β} secondary shifts measured for βS correlate well with the structural propensities at the N and C terminus of the protein (Supplementary Data, Figure S1B). When the ^{15}N amide secondary shifts were evaluated, negative deviations were observed at the N terminus, indicative of α-helical propensities, whereas positive deviations were predominantly located at the C terminus, indicative of extended β conformations and polyproline II structures (Supplementary Data, Figure S1C). Added to these experimental evidences is the occurrence of eight proline residues at the C terminus domain, known to impede β-sheet formation, that could impose local restrictions favoring the population of conformations with polyproline II contents.

We observed that hydrophilic regions at the N terminus of the protein displayed propensity to adopt α-helical conformation, while hydrophobic regions reflected tendency to populate conformations with residual β-sheet character, likely providing a minimized interaction with the polar solvent (Figure 3(c)). The correlation with the solvent is lost for the C terminus of the protein. Due to the high net charge of this region (−16), a strong hydrophilicity is predicted, but as mentioned above the chemical shift analysis indicates an overall tendency to populate the β-space of the Ramachandran map. We interpret this observation as a tendency to adopt polyproline II conformations, where the helical nature of this particular structure will thus be in line with the hydrophilic properties of the C terminus.

To shed more light on the structural propensities of βS, particularly at the C terminus, we measured three bond HN–Hα coupling constants ($^{3}J_{HNH\alpha}$), which are useful indicators of the ϕ torsion angle populated by each residue. This coupling is in the order of 3–5 Hz for a helical structure (including α-helix and polyproline II) and 8–11 Hz for a β-sheet structure.[29] For a random coil, a weighted average of these values would be observed, which is typically between 6.0 and 8.0 Hz for most residues. Similarly to secondary chemical shifts (Δδ), deviations of the observed coupling constant from the random coil value (J_{obs}–J_{rc}),[29,30] called secondary coupling constants, provide valuable light on the

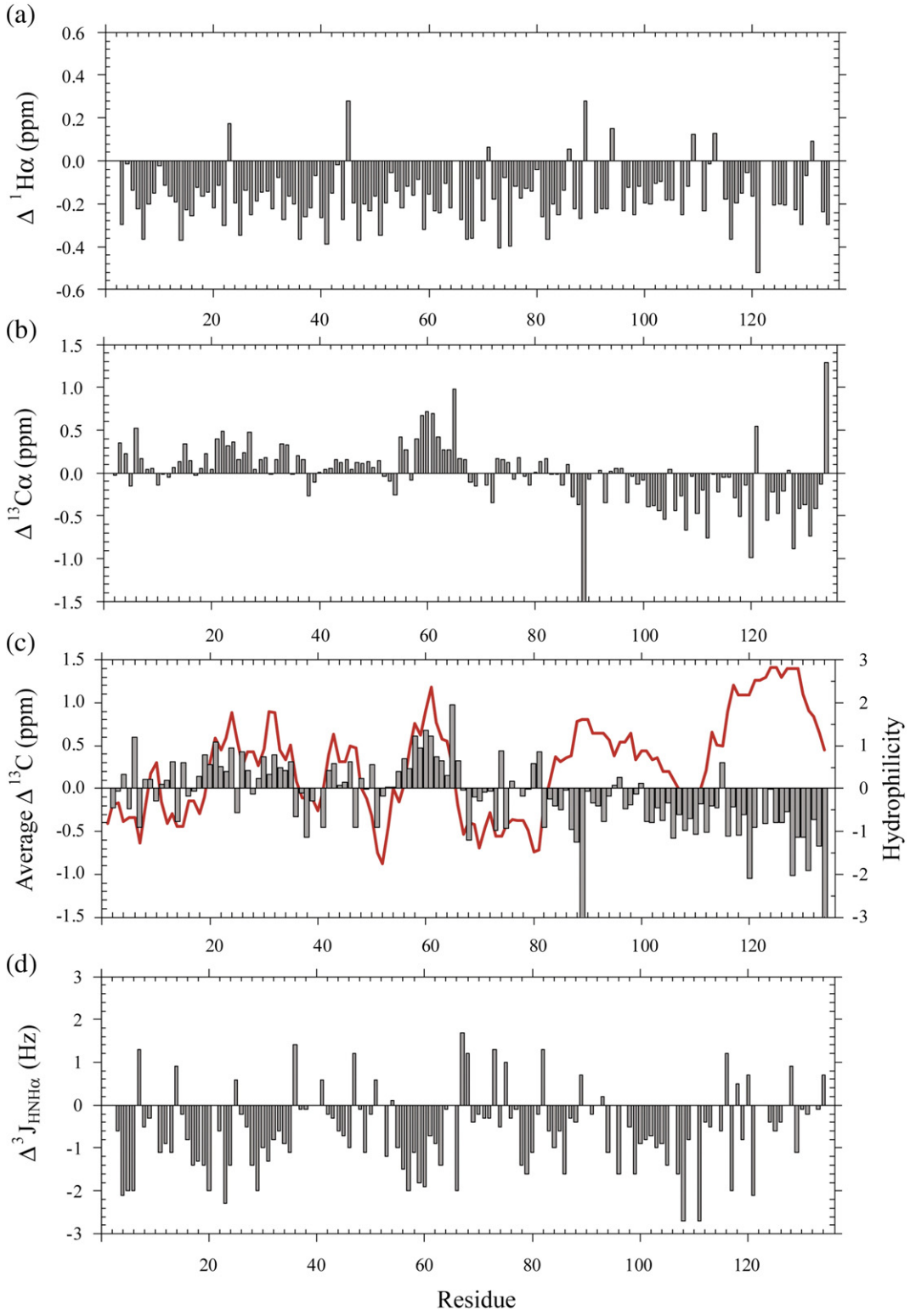

Figure 3. Structural propensities for the backbone of βS. The measured chemical shifts for backbone $^{1}H^{\alpha}$ and ^{13}C atoms of βS were subtracted from random coil values and the differences (secondary shifts) are plotted. (a) H^{α} atoms; (b) C^{α} atoms; (c) weighted C′ and C^{α} atoms (bars) are depicted together with the predicted hydrophilicity (red line, five residue window). The average shifts were calculated as $[3\Delta\delta(C^{\alpha})+4\Delta\delta(C')]/7$. (d) Three-bond scalar coupling between amide and alpha protons ($^{3}J_{HNH\alpha}$), indicative of the ϕ torsion angle. Secondary couplings (J_{obs}–J_{rc}) are plotted (see Materials and Methods for details).

secondary structural propensities along the polypeptide chain. Negative secondary coupling constants would indicate helical propensities (including polyproline II) and positive secondary coupling constants would indicate β-sheet propensities. The measured values of the secondary $^{3}J_{HNH\alpha}$ coupling

constants for βS in solution are plotted in Figure 3(d) and Supplementary Data, Figure S2. Interestingly, the regions exhibiting the highest positive C^{α} and C′ deviations at the N terminus (Figure 3(b) and (c)) showed also the strongest negative secondary coupling constants, in agreement with the predominant α-helical propensities suggested for this domain. Instead, C-terminal regions exhibited predominance of negative deviations for both C^{α} and C′ and positive deviations for the ^{15}N secondary shifts. Combined to these results, the measurement of negative secondary coupling constants at the C terminus strongly suggest that their backbone ϕ, ψ values might populate polyproline II structures.

Comparison of αS and βS structural propensities

In order to compare the structural propensities determined for the ensemble of conformations of βS with that of αS we measured the whole set of NMR parameters for the latter protein under the same experimental conditions. From the qualitative analysis of the secondary chemical shifts and coupling constants a strong correlation is observed on the structural propensities along the N terminus of both proteins, reflecting the high degree of homology at this domain (Figure 4). However, subtle differences were observed when the magnitude of the secondary parameters characterizing the 20–35 and 55–65 regions in βS were compared with αS. Whereas a clear difference is observed in the magnitude of the secondary $^{3}J_{HNH\alpha}$ coupling constants for both proteins within the 20–35 region (Figure 4(c)), indicative of a higher degree of helical propensity in βS, these differences seem to be obscured at the chemical shift level (Figure 4(a) and (b)). Since the latter parameter is much more sensitive to environmental effects, the discrepancies might be derived from the effect induced by the long-range (electrostatic) interactions between the N and C-terminal regions in αS.[16] By contrast, the magnitude of both secondary chemical shifts and coupling constants parameters evidenced a higher propensity to adopt α-helical conformations in the 55–65 region of βS compared to αS. In this case, the different degree of homology between the stretches, the lack of an hydrophobic environment provided by the central region of βS (amino acid residues 71–82 in αS) or a combination of both factors might contribute to stabilize the transient α-helical structures.

A recent structural study on γ-synuclein (γS) reported an increased α-helical structure in the amyloid-forming region (amino acid residues 39–90) of that protein when compared to αS.[31] Such differences were attributed to the absence of tertiary contacts involving the C terminus of γS, similarly to what we found in βS. The same study predicted that βS would have the highest α-helical propensity for the region 39–90 (βS>γS>αS), as supported by our measurements (Figure 4). It is then probable that the absence of the central hydrophobic cluster in βS (amino acid residues 71–82), present in αS and γS, might contribute to stabilize locally encoded α-helical conformations at the N terminus.

At the C terminus, the NMR-derived structural parameters show striking similarities in the secondary C^{α} and C′ chemical shifts of αS and βS, whereas the ^{15}N secondary shifts and the secondary $^{3}J_{HNH\alpha}$ couplings suggest a propensity to polyproline II structures in βS (Figure 4). This denote that the combined analysis of ^{15}N chemical shifts and $^{3}J_{HNH\alpha}$ scalar coupling constants are an excellent tool for identifying polyproline II conformations, as suggested by Lam & Hsu.[32] Since the predicted negative charge of the C-terminal domain is similar for both proteins (−14 in αS and −16 in βS), differences in the content of proline residues (five in αS and eight in βS) and the lack of tertiary long-range contacts in βS would be likely the main contributors to this differential picture.[16]

Since αS fibrillation is believed to progress through a soluble oligomeric intermediate rich in β-structure,[33] the differences in secondary structure propensity between αS and βS might provide a possible explanation for their different amyloidogenic potential. The increased α-helical propensity, added to the lack of the central hydrophobic cluster in βS might stabilize the intrinsically disordered state relative to the β-structured intermediate, thus inhibiting oligomerization. Interestingly, a strong correlation was found between the predicted helicity in the amyloid forming region of synucleins and their relative fibrillation propensities.[31] For example, the A53T mutant of αS, which was reported to fibrillate faster than the wild-type protein, shows a lower predicted helicity compared to αS. On the other hand, βS which has the highest predicted helicity (βS>γS>αS>A53T) possess the lowest fibrillation propensity (A53T>αS>γS>βS).[31]

Regarding to the specific anti-amyloidogenic properties shown by βS and not by αS and γS, the propensity to populate polyproline II conformation found in βS might play a relevant role. The extended conformation and flexibility of polyproline II serve as a scaffold for the interaction with target proteins and might be then involved in the molecular recognition step with αS. Although the nature of the conformational effect induced by βS on αS, and the precise contribution of each structural element to that process are not revealed by the data presented here, an appealing mechanism would involve βS interfering with the nucleation process, perhaps by maintaining αS in an aggregation-incompetent conformation. The target of such a molecular recognition event may either be an aggregation prone monomer of αS, where hydrophobic residues in the NAC region are solvent exposed, or oligomeric forms of the protein. A capping mechanism of nascent fibrils, by the addition of βS monomers to the ends of actively growing proto-filaments of αS could also

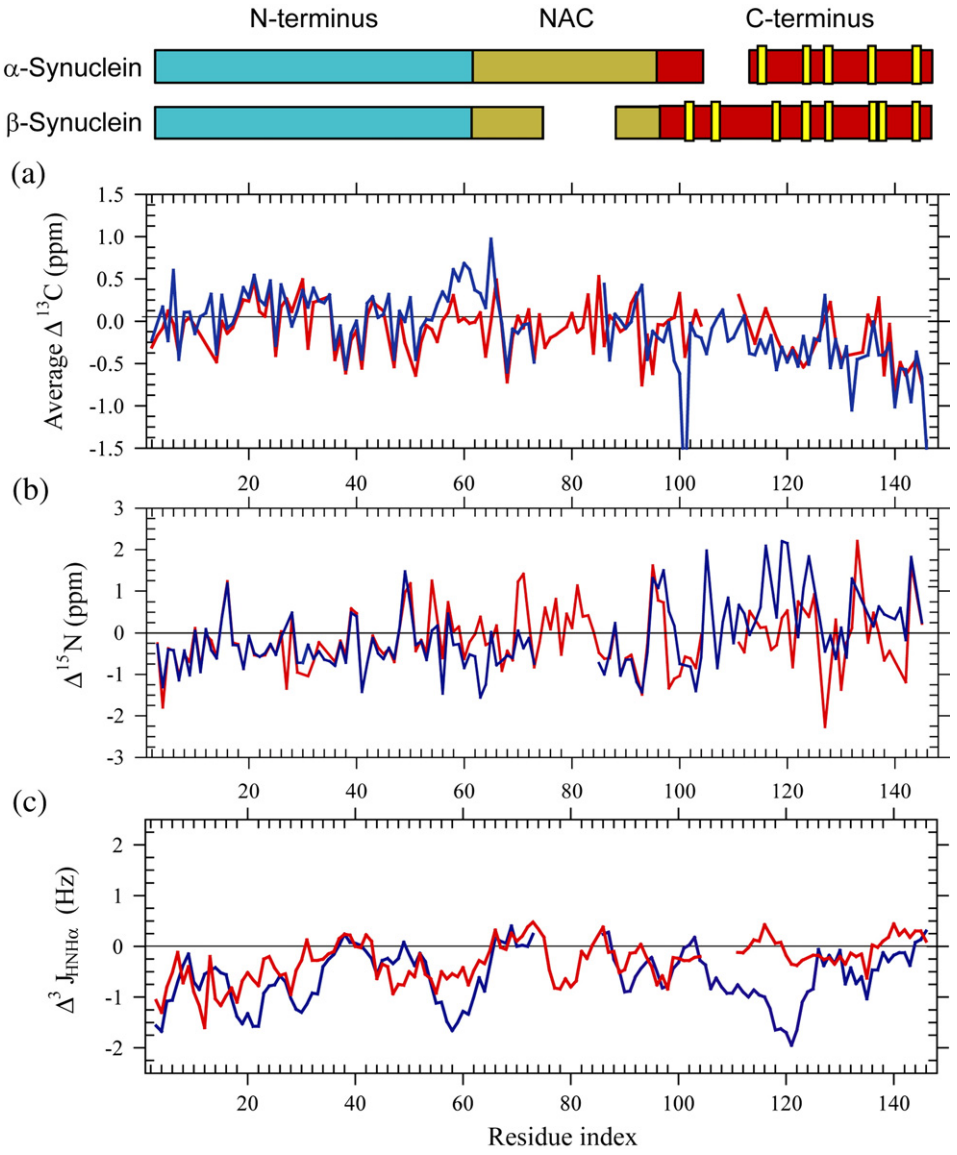

Figure 4. Comparison of secondary structure propensities in αS and βS. In red is shown αS and in blue βS, aligned according to the lack of the NAC region in βS and the shorter C terminus in αS (top scheme). The position of proline residues is indicated in yellow. (a) Mean weighted ^{13}C chemical shifts deviations for αS and βS, indicative of secondary structure propensities for the polypeptide backbone. (b) ^{15}N chemical shifts deviations for αS and βS. (c) $^{3}J_{HNH\alpha}$ deviations from random coil values in αS and βS (see Materials and Methods for details).

be a third plausible mechanism for the inhibitory process.

Residual structure in βS is locally encoded

Residual dipolar couplings (RDCs) are a very powerful NMR parameter to characterize and refine the structure of globular proteins since they report on the orientation of the inter-nuclear bond vector with respect to the molecular axis.[34] In the case of highly populated unfolded states, RDCs have been successfully applied to uncover conformational restrictions and characterize residual structural elements on many proteins.[35–37] Interpretation of RDCs in random coil polypeptides has been a subject of debate,[38,39] but we recently showed that they report on the degree of local conformations dictated largely by the amino acids bulkiness profile in the region.[40,41] Such deviations from the random coil behavior can provide further insights into residual secondary structure and long-range transient interactions in weakly structured proteins. We have previously applied this technique to characterize the native state of αS and revealed the existence of residual structure elements at the C terminus that are crucial for inhibiting protein aggregation.[16] When one-bond N-H dipolar couplings (D_{NH}) were measured in βS aligned in C_8E_5/octanol as anisotropic media, we observed predominantly positive couplings, similar to that described for αS (Figure 5(a)). However, a particular feature observed in the βS RDCs profile are the high values at the whole C terminus of the protein, corresponding on average to twice the values measured at the N terminus and suggesting a significant amount of

residual structure in the region. Furthermore, a poor agreement between bulkiness and the N-H RDCs is found for the whole C terminus in βS (Figure 5(b)), supporting the occurrence of residual structure in this domain.[41] Importantly, the general features of the RDCs in βS were reproduced in a second independent alignment media, employing Pf1 phages to obtain the anisotropic phase (Supplementary Data, Figure S3).

To evaluate the contribution of local and non-local interactions in the stabilization of the residual structure observed at the C terminus of βS, we employed paramagnetic relaxation enhancement (PRE) by nitroxide spin labels to study the conformations populated by βS in solution (Figure 6). When the paramagnetic probe was located at the N terminus of the protein (position 18) the broadening effect was mainly local although it spread beyond what is expected for a random coil polypeptide, likely suggesting some degree of compactness in the region (Figure 6(a) and (c)). This is consistent with the population of helical structures in the regions 20–35 and 55–65 of the N terminus. When the spin labeling was placed towards the end of the central domain (position 79), the paramagnetic effect was slightly extended towards the N terminus of the protein but no effect was observed towards the C terminus (Figure 6(b) and (d)). Paramagnetic labeling at the 18 and 79 positions in βS mirrors the 18 and 90 positions employed in the study of αS, which allowed us to demonstrate the occurrence of long-range contacts between the N and C terminus of the protein and the compaction at the C terminus driven by its interaction with the central hydrophobic stretch.[16] Based on the results shown here, βS is not only devoid of long-range interactions but also no compaction is evident at the C terminus, in line with the extended nature of the polyproline II conformation. These findings strongly suggest: (i) a key role for the NAC domain as the main driving force for the stabilization of the ensemble of auto-inhibited conformations adopted by αS; (ii) that the residual polyproline II structure identified at the C terminus of βS would be exclusively determined by locally encoded conformational restrictions; (iii) that the abundant proline residues distributed along the region together with side-chain–side-chain repulsions would be the main factors determining the residual structure at the C terminus of βS.

Polyproline II structuring at the C terminus of βS occurs in the nano to microseconds timescale

Whereas RDCs probe both structure and dynamics, heteronuclear relaxation rates monitor directly backbone motional restrictions. ^{15}N R_1 and R_2 relaxation and heteronuclear nuclear Overhauser

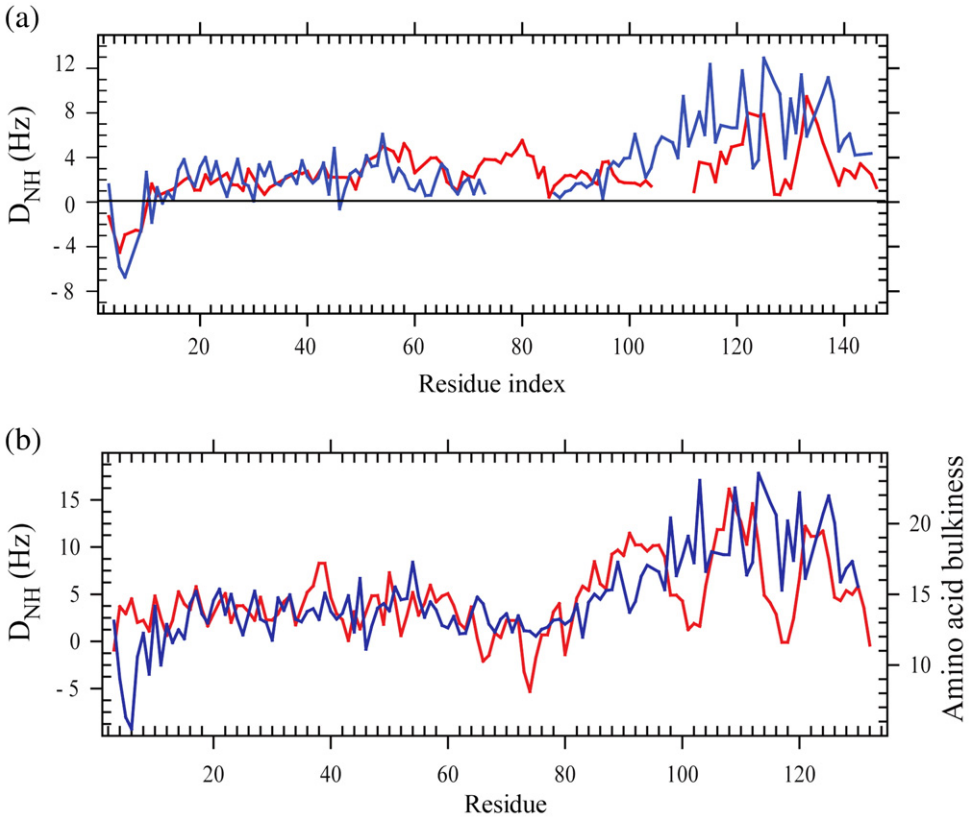

Figure 5. Comparison of residual dipolar couplings between αS and βS. (a) ^{1}H-^{15}N backbone RDCs profile for αS (red) and βS (blue) aligned in 5% C_8E_5/octanol. Measurement conditions were pH 6.5 and 100 mM NaCl in all experiments. Importantly, the main features of the RDCs pattern were reproduced in Pf1 as a second alignment media (Supplementary Data, Figure S3). (b) Comparison between amino acid bulkiness (five residue averaged window)[41] and N-H RDCs for βS.

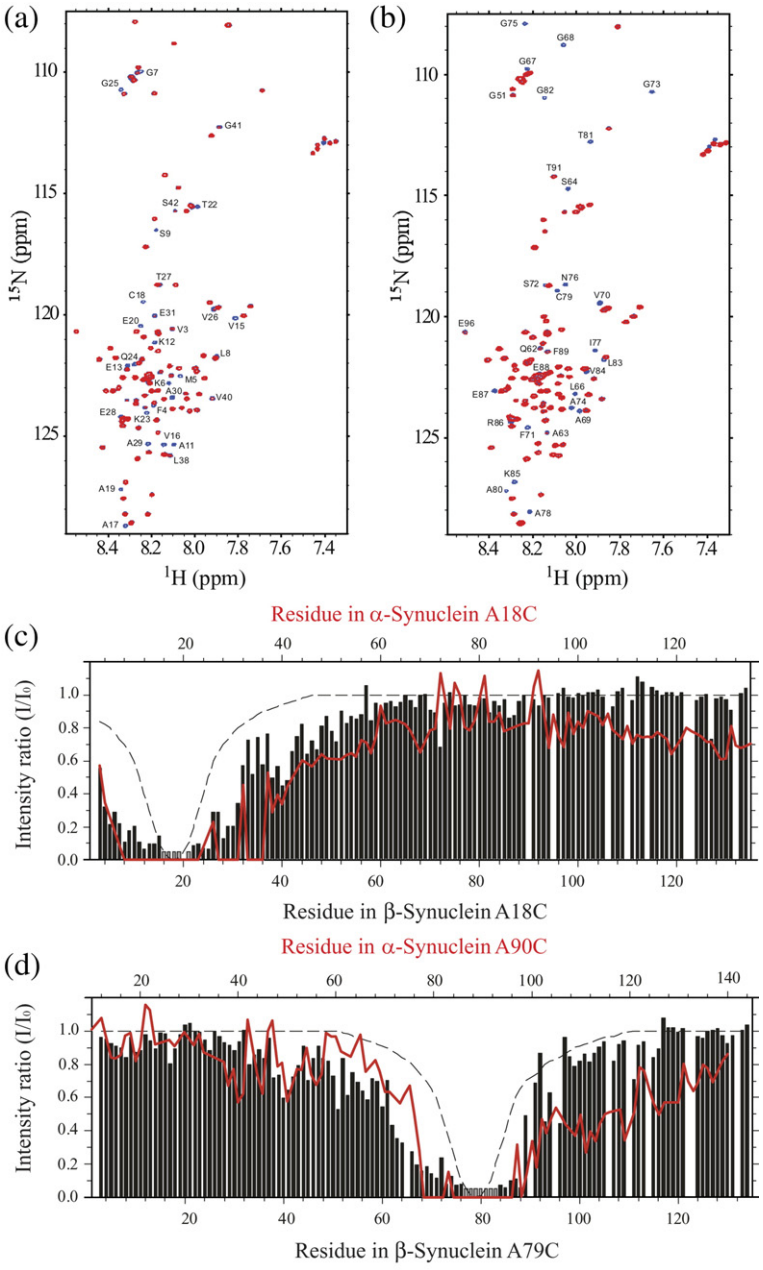

Figure 6. Paramagnetic relaxation enhancement in βS. Two Cys-containing mutants of βS (A18C and A79C) were constructed in order to provide attachment sites for the long-range paramagnetic probe MTSL. (a) Overlay of the ^{1}H-^{15}N HSQC spectra measured in the presence (red) and absence (blue) of MTSL attached to position 18. Note how affected resonances are broadened beyond detection. (b) Same as (a), but for the MTSL tag located at position 79. (c) Profile of intensity ratios for amide resonance peaks between the paramagnetic (I) and diamagnetic (no I_o) states for βS-A18C protein (black bars). In red, the intensity ratios for the mirrored mutant in αS (αS-18C) are overlaid for comparison. The expected profile for a random coil polypeptide, with the paramagnetic tag at the same position, is depicted in grey broken line. (d)The same as (c), but for βS-A79C (black bars) and αS-A90C (red line).

enhancements (NOEs) for the backbone amide resonances of βS are shown in Figure 7. NOEs are very sensitive to picoseconds timescale motions, while R_2 values are sensitive to micro- to millisecond timescale motions (conformational transitions) and the R_1 values are sensitive to both high and low frequency motions (pico- to nanoseconds timescale motions).[42] Clearly, the relaxation parameters observed for βS are consistent with the intrinsically unfolded nature of the protein. For R_1 measurements, a mean value of 1.4 s^{-1} was observed (Figure 7(a)), while the average R_2 value was 3.0 s^{-1} (Figure 7 (b)), very similar to the relaxation rates reported for αS[18] and other native unfolded polypeptides as the HIV-1 Tat protein or the histone mRNA binding protein SLBP.[43,44] The heteronuclear NOE intensity for the whole backbone varies from −0.2 to 0.2, indicative of the absence of restricted dynamics in the ps–ns timescale.

The bell-shaped relaxation profiles showed larger variations in the R_2 rates, in agreement with previous studies on unstructured polypeptides.[45] The most important R_2 deviation is located at the N terminus of βS, clustered in the sequence connecting the two neighboring regions showing α-helical propensities in the native state of βS (amino acid residues 20–35 and 55–65). Interestingly, the α-helix at the N-terminal domain of βS in its micelle-bound form was recently shown to be clearly interrupted around position 42.[46] Although more evidences are clearly needed, the decreased helical propensity revealed by the chemical shift profile and the substantial deviation of the R_2 rates in that region might be suggesting that the manner in which the protein interact with

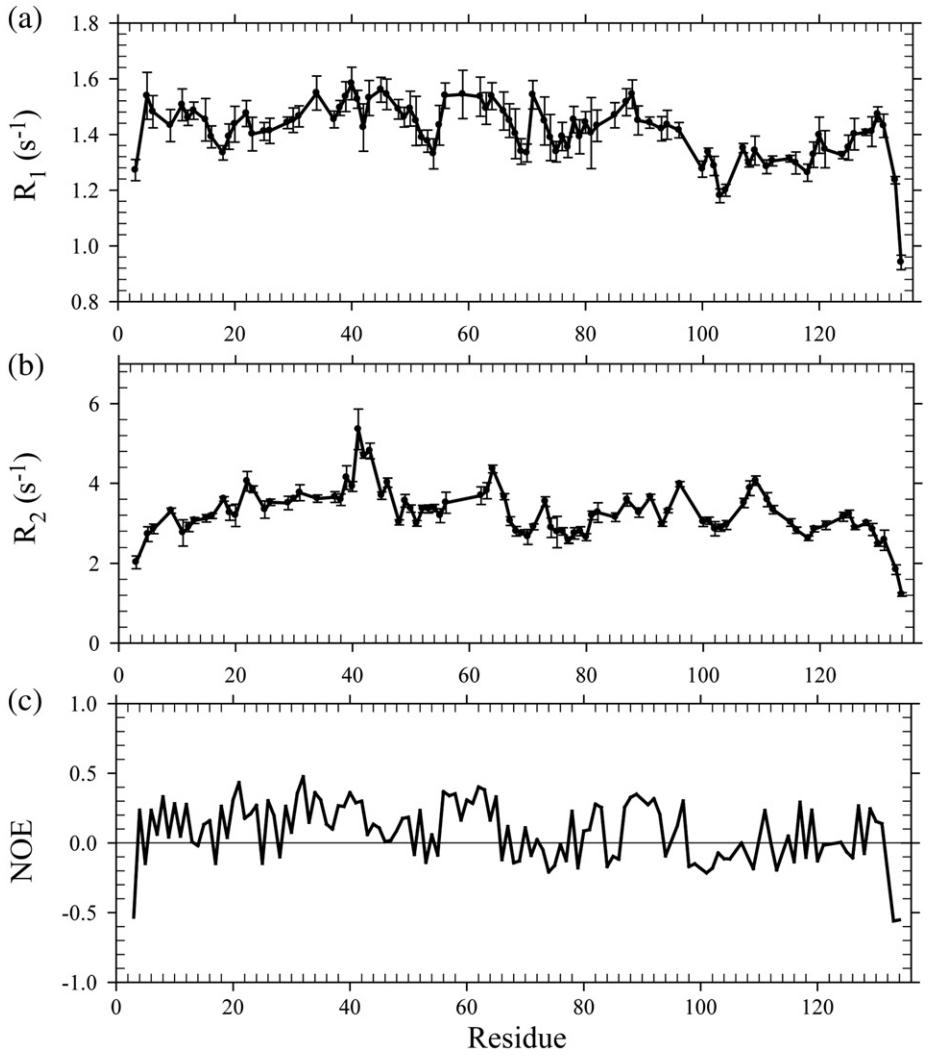

Figure 7. ^{15}N NMR backbone relaxation in βS. (a) Longitudinal relaxation rates (R_1); (b) transverse relaxation rates (R_2); (c) heteronuclear NOEs.

membranes would be already encoded in its disordered solution state.

Altogether our data suggest that the interconversion among conformers of high and low polyproline II structural content in βS occurs on a ns to μs timescale, which have been successfully probed only by RDCs. We and others have recently shown the ability of RDCs to reveal slow dynamics and backbone structuring in unfolded proteins, demonstrating that they report on averages over longer time scales (up to the ms range) and therefore encode key information for understanding protein motions in the submicro- to millisecond range.[47,48] The evidence shown here is then another example of the potential of RDCs to characterize both the structure and dynamics of unfolded states of proteins.

Polyproline II in βS: structural, functional and biological implications

From the few biophysical studies focused on the structural features of native βS, Raman optical activity (ROA) measurements suggested that the major conformational element present in all three synucleins is the polyproline II helix,[49] whereas CD studies failed to detect any polyproline II conformational propensity in these proteins.[11] The ^{15}N secondary shifts and $^{3}J_{HNH\alpha}$ coupling values reported here were able to identify polyproline II conformations in βS, locally restricted to the C-terminal region.

The lack of a positive band around 218–222 nm in the CD spectrum of βS does not necessarily indicate the absence of polyproline II content, since the conformational averaging resulting from the presence of other local structures might lead to changes in ellipticity in that region. More conclusive is the picture obtained from the comparison of the results measured by ROA[49] and NMR spectroscopies. The ^{15}N chemical shifts, $^{3}J_{HNH\alpha}$ coupling constants and ROA determinations report on the local, short-range structure of the protein and contain little information on the long-range structure or the correlation between different segments of local structure. However, for the full description of a flexible protein

one needs to consider both short and long-range structural information. Indeed, from the ROA based studies it can be concluded that the structure of βS would exhibit significant fluctuations around the ideal polyproline II helix. By contrast, the dynamics and structural heterogeneity present in βS combining short- ($\Delta\delta$ and $\Delta^3J_{HNH\alpha}$) and long-range (R_H and PRE measurements) sensitive NMR parameters indicate that the native state of βS would not be the sum of local polyproline II helices, but is an ensemble of inter-converting conformations that prefer locally a broad basin around α-helix (N terminus) and polyproline II (C terminus) geometries, but globally has to be represented by something akin to a random walk. In view of the conflicting evidence as to the role of polyproline II conformation in unfolded states of proteins, our results support the hypothesis that polyproline II conformation would be one of the sterically feasible and favorable states in the ensemble adopted by intrinsically unfolded proteins, rather than a general feature of their interconverting states.[50–56]

The analysis of the primary sequence of the C terminus of βS reveals not only a larger number of proline residues than those found in αS but a particularly distinctive distribution of some of these residues along the region. Indeed, the region 105–115 is characterized by the presence of the motif EPLXEPLXEPE, that resemble the proline-rich sequences of proteins implicated in synaptic vesicle endocytocis and vesicle trafficking processes.[57,58] Then, the presence of proline residues and the stabilization of polyproline II conformations in βS might be related to a functional role in the protein. In the case of αS, proline residues are mainly located at the 115–130 region of the C terminus, characterized by the presence of two hydrophobic clusters, 115–119 (Met116-Pro117) and 125–129 (Met127-Pro128), corresponding to structural elements with restricted motional properties that are critically stabilized by long-range interactions with the central NAC region.[16,17] Then, the strategic location of prolines in αS seems to play a structural role, contributing to increase the conformational restrictions in the region and stabilizing the native state of αS.

From the biological point of view, the extended conformation and flexibility of the polyproline II structure may also serve as a scaffold for the interaction with target proteins. This might well be the reason for the specific anti-amyloidogenic properties displayed by βS, and not by αS or γS, as suggested above. Indeed, in some patients with DLB it has been recently found in βS a proline to histidine substitution at position 123. The P123H missense mutation has been characterized as autosomal dominant with a reduced penetrance, displaying extensive αS aggregation.[59] In light of our study it is very likely that the change of the small, uncharged, and sterically constrained proline residue by the polar, bulky, and flexible histidine would disfavor the persistence of polyproline II conformations, possibly affecting βS anti-amiloydogenic function.

Extended polyproline II conformation is also becoming increasingly associated to protein misfolding, as it has been reported for the Aβ peptide,[60] lysozyme,[61] poly(Q) tracts[62] and phosphorilated Tau.[63] On the other hand, it has been recently observed for Aβ and poly(Q) that the C-terminal addition of a 10- mer polyproline peptide (P10) suppresses aggregation, probably by stabilizing an aggregation-incompetent conformation of the monomer.[64] Our structural characterization of βS foresees a similar mechanism for the inhibition of αS aggregation which still remains to be proven experimentally, suggesting that polyproline II could not only be the culprit but also may be a savior in protein misfolding. Ongoing solution structural studies will provide further insight into the mechanism of βS effect on αS conformation and aggregation.

Materials and Methods

Protein preparation

αS and βS were expressed in *Escherichia coli* BL21 cells grown in M9 minimal medium supplemented with $^{15}NH_4Cl$ or $^{15}NH_4Cl$ and D- [^{13}C]glucose (Cambridge Isotope Laboratories) and were purified under the same protocol as described for αS.[65] Purified proteins were dialyzed against buffer A (20 mM Mes (pH 6.5), 100 mM NaCl).

Construction of βS cysteine-containing mutants

The Ala18Cys and Ala79Cys βS cysteine-containing mutants were constructed using the Quick-Change site directed mutagenesis kit (Stratagene) on the βS containing plasmid, with the use of the following primers:

βS-A18C-Fwd: 5′-gagggcgttgtggcatgcgcggagaaaaccaag-3′
βS-A18C-Rev: 5′-cttggttttctccgcgcatgccacaacgccctc-3′
βS-A79C-Fwd: 5′-gcagggaacatcgcatgcgccacaggactggtg-3′
βS-A79C-Rev: 5′-caccagtcctgtggcgcatgcgatgttccctgc-3′

The introduced modifications were further verified by DNA sequencing. The cysteine replacements mirror the ones employed for αS studies,[16] and were selected to report long-range interactions between the N terminus and C terminus of the protein. The introduction of these mutations did not cause chemical shifts changes besides the residues surrounding the point of mutation. Mutant βS proteins were produced by the same procedure as the wild type protein, but 1 mM DTT was included throughout the different purification steps.

Spin-labeling of βS

The reaction of βS cysteine-containing mutants with the nitroxide spin label (1-oxy-2,2,5,5-tetramethyl-D-pyrroline-3-methyl)-methanethiosulfonate; (MTSL; Toronto Research Chemicals, Toronto, Ontario, Canada) was carried out as described.[16] Diamagnetic samples were measured after the paramagnetic sample by removing the tag with the addition of 0.5 mM DTT.

Alignment of αS and βS in anisotropic media

One-bond N–H residual dipolar couplings (D_{NH}) were measured in αS and βS aligned in 10 mg/ml bacteriophage Pf1 (Asla, Riga, Latvia)[66] and in 5% (w/v) *n*-octylpenta(ethylene glycol)/octanol (C_8E_5) (Sigma).[67]

NMR measurements

NMR spectra were acquired at 15 °C on Bruker Avance 600, Avance II 600 and Avance 900 MHz NMR spectrometers (Avance spectrometers were equipped with cryoprobes). Pulse field gradient NMR experiments for αS and βS were acquired at 15 °C on a 200 μM unlabeled protein sample dissolved in 99.9% ^2H_2O, 20 mM phosphate buffer (pH 6.5) (uncorrected), 100 mM NaCl, and containing dioxane (~20 mM) as an internal radius standard and viscosity probe.[20] Deuterium oxide was employed instead of water in order to minimize the power level necessary for water pre-saturation. Twenty one-dimensional ^1H spectra were collected as a function of gradient amplitude employing the PG-SLED sequence.[68] The gradient strength was shifted from 1.69 Gauss cm^{-1} to 33.72 Gauss cm^{-1}, in a linear manner. Each ^1H spectrum comprised 32 scans plus 16 steady-state scans. Sixteen K complex points were acquired with a spectral width of 6000 Hz. The signals corresponding to the aliphatic region of the ^1H spectra (3.3 ppm–0.5 ppm) were integrated and the decay of the signal as a function of the gradient strength was fitted to a Gaussian function to determine d^{prot}. The same procedure was applied for the dioxane peak (~3.6 ppm) and the d^{ref} was measured. The R_H for the protein was calculated from the known R_H (2.12 Å) for the dioxane and the ratio between the measured d^{ref}/d^{prot}.

The following three-dimensional triple-resonance experiments were collected to obtain sequence-specific assignments for the backbone of βS: HNCACB, CBCACONH, HNCO, HN(CA)CO, HNN and HNHA. Acquisition parameters for the triple resonance experiments were as follows: HNCACB: field (MHz): 600; real points: 40 (^{15}N), 70 (^{13}C), 1024 (^1H); spectral width (ppm): 23 (^{15}N), 60 (^{13}C), 9 (^1H). CBCACONH: 900; 35, 60, 1024; 23, 60, 9. HNCO: 900; 45, 25, 1024; 22, 8.8, 9. HNCACO: 900; 64, 40, 1024; 22, 8.8, 9. HNN: 900; 35, 62 (^{15}N), 1024; 23, 23 (^{15}N), 9. HNHA: 900; 60, 128 (^1H), 1024; 26, 9 (^1H), 9. All these experiments were acquired at 15 °C on a 400 μM protein sample in buffer A. Secondary shift values were calculated as the differences between the measured $H^\alpha/CO/C^\alpha/C^\beta$ chemical shifts and the empirical random coil values reported by Wishart *et al.*[27] Random coil values from Lam and Hsu[32] were employed for the calculation of ^{15}N secondary shifts. DSS was employed for indirect chemical shift referencing.

Three bond HN–H^α coupling constants $^3J_{HNH\alpha}$ were determined from the ratio between the intensities of the diagonal and cross-peak in the HNHA experiment, according to the relation Intensity (cross-peak) / Intensity (diagonal peak) = $-\tan^2(2\pi\varepsilon J_{HNH\alpha})$. For calculation of secondary coupling constants (J_{obs}–J_{rc}), random coil values for each amino acid were subtracted from the experimental values. Two sets of random coil $^3J_{HNH\alpha}$ couplings were evaluated, the ones reported by Serrano[29] (Figures 3(d) and 4(c)), and the ones reported by Smith *et al.*[30] (Supplementary Data, Figure S2). For the profiles of $^3J_{HNH\alpha}$ comparing αS and βS (Figure 4(c)), a five residue window averaging was employed to minimize contributions of local variations in the sequence of both polypeptides.

^{15}N relaxation data were acquired with modern versions of pulse sequences based on those described by Farrow *et al.*[69] Spectra used for longitudinal relaxation R_1 analysis were collected using the following relaxation delay times (in ms): 20, 100, 200, 500, 1000, and 20. R_2 data were measured using a pulse sequence employing a CPMG pulse train with the following relaxation delays (in ms): 3.8, 19, 38, 57, 114, 228, 3.8, and 228. Duplicate spectra were collected at several time points to estimate uncertainty. The delay between 180° pulses in the CPMG pulse train was ~1 ms. Resonance heights were extracted and fit as a function of the relaxation delay time using SPARKY routines in order to determine R_1 and R_2 relaxation rates. Steady-state NOE values are reported as the ratio of peak heights in paired spectra collected with and without an initial period (4 s) of proton saturation during the 5s recycle delay.

Paramagnetic relaxation enhancement by nitroxide spin labels in βS Cys-containing mutants were measured as ratios of peak intensity between two two-dimensional ^1H-^{15}N HSQC NMR spectra, in the presence and absence of the nitroxide radical. Spectra were recorded using 256 × 1024 complex data points in *F*1 and *F*2 dimensions with 16 scans per increment and a relaxation delay of 1.2 s. The removal of the spin label for measurement of the diamagnetic state was accomplished by addition of 0.5 mM DTT to the protein solution and 30 min incubation at room temperature.

One-bond N–H RDCs (D_{NH}) were determined using the IPAP ^{15}N-HSQC sequence.[70] D_{NH} values were calculated as the difference between splittings measured in an aligned sample and those measured in an isotropic sample, and were not corrected for the negative gyromagnetic ratio of ^{15}N. RDCs observed for βS were normalized according to the size of the splitting of the deuterium signal for RDCs measured for αS under the same alignment conditions. Bulkiness in βS was computed as described by Cho *et al.*[41]

The same experimental conditions were employed to measure backbone chemical shifts, $^3J_{HNH\alpha}$ couplings and RDCs on αS.

All spectra were processed and analysed using nmrPipe[71] and SPARKY†.

Deposited data

The backbone assignment of βS containing $^1H\alpha$, ^1HN, ^{15}N, ^{13}CO, $^{13}C^\alpha$, and $^{13}C^\beta$ chemical shifts has been deposited at the Biological Magnetic Resonance Data Bank‡ under number 15298.

Acknowledgements

C.O.F. thanks ANPCyT, Fundación Antorchas, Max Planck Society and the Alexander von Humboldt Foundation for financial support. C.O.F. and R.M.R. are staff members of CONICET (Argentina). C.O.F. is the head of a Partner Group of the Max Planck Institute for Biophysical Chemistry (Göttingen).

† Goddard, T. D. & Kneller, D. G. SPARKY 3. University of California, San Francisco.

‡ http://www.bmrb.wisc.edu/

At the moment of the research C.W.B. was supported by a fellowship from the DFG Center for Molecular Physiology of the Brain (CMPB) in Göttingen, and R.M.R. was recipient of a fellowship from AvH Foundation. C.W.B acknowledges EMBO for a long term fellowship. A.B. is recipient of a fellowship from ANPCyT in Argentina. G.R.L. is recipient of a fellowship from CONICET in Argentina. M.Z. acknowledges a Heisenberg grant (ZW 71/2-1- and 3-1). This work was supported by the CMPB, the DFG and the Max Planck Society. The Bruker Avance II 600 MHz NMR spectrometer used in this work was purchased with funds from ANPCyT (PME2003-0026) and CONICET.

Supplementary Data

Supplementary data associated with this article can be found, in the online version, at doi:10.1016/j.jmb.2007.07.009

References

1. Dyson, H. J. & Wright, P. E. (2005). Intrinsically unstructured proteins and their functions. *Nature Rev. Mol. Cell. Biol.* **6**, 197–208.
2. Uversky, V. N. (2002). Natively unfolded proteins: a point where biology waits for physics. *Protein Sci.* **11**, 739–756.
3. Sherman, M. Y. & Goldberg, A. L. (2001). Cellular defenses against unfolded proteins. A cell biologist thinks about neurodegenerative diseases. *Neuron*, **29**, 15–32.
4. Dobson, C. M. (2003). Protein folding and misfolding. *Nature*, **426**, 884–890.
5. Clayton, D. F. & George, J. M. (1998). The synucleins: a family of proteins involved in synaptic function, plasticity, neurodegeneration and disease. *Trends Neurosci.* **21**, 249–254.
6. Buchman, V. L., Hunter, H. J., Pinon, L. G., Thompson, J., Privalova, E. M., Ninkina, N. N. & Davies, A. M. (1998). Persyn, a member of the synuclein family, has a distinct pattern of expression in the developing nervous system. *J. Neurosci.* **18**, 9335–9341.
7. Chandra, S., Gallardo, G., Fernandez-Chacon, R., Schluter, O. M. & Sudhof, T. C. (2005). Alpha-synuclein cooperates with CSPalpha in preventing neurodegeneration. *Cell*, **123**, 383–396.
8. Spillantini, M. G., Schmidt, M. L., Lee, V. M., Trojanowski, J. Q., Jakes, R. & Goedert, M. (1997). Alpha-synuclein in Lewy bodies. *Nature*, **388**, 839–840.
9. Volles, M. J. & Lansbury, P. T. (2003). Zeroing in on the pathogenic form of alpha-synuclein and its mechanism of neurotoxicity in Parkinson's disease. *Biochemistry*, **42**, 7871–7878.
10. Hashimoto, M., Rockenstein, E., Mante, M., Mallory, M. & Masliah, E. (2001). beta-Synuclein inhibits alpha-synuclein aggregation: a possible role as an anti-parkinsonian factor. *Neuron*, **32**, 213–223.
11. Uversky, V. N., Li, J., Souillac, P., Millett, I. S., Doniach, S., Jakes, R. *et al.* (2002). Biophysical properties of the synucleins and their propensities to fibrillate: inhibition of alpha-synuclein assembly by beta- and gamma-synucleins. *J. Biol. Chem.* **277**, 11970–11978.
12. Rockenstein, E., Hansen, L. A., Mallory, M., Trojanowski, J. Q., Galasko, D. & Masliah, E. (2001). Altered expression of the synuclein family mRNA in Lewy body and Alzheimer's disease. *Brain Res.* **914**, 48–56.
13. Hashimoto, M., Rockenstein, E., Mante, M., Crews, L., Bar-On, P., Gage, F. H. *et al.* (2004). An antiaggregation gene therapy strategy for Lewy body disease utilizing beta-synuclein lentivirus in a transgenic model. *Gene Ther.* **11**, 1713–1723.
14. Park, J. Y. & Lansbury, P. T., Jr (2003). Beta-synuclein inhibits formation of alpha-synuclein protofibrils: a possible therapeutic strategy against Parkinson's disease. *Biochemistry*, **42**, 3696–3700.
15. Dyson, H. J. & Wright, P. E. (2004). Unfolded proteins and protein folding studied by NMR. *Chem. Rev.* **104**, 3607–3622.
16. Bertoncini, C. W., Jung, Y. S., Fernandez, C. O., Hoyer, W., Griesinger, C., Jovin, T. M. & Zweckstetter, M. (2005). Release of long-range tertiary interactions potentiates aggregation of natively unstructured alpha-synuclein. *Proc. Natl Acad. Sci. USA*, **102**, 1430–1435.
17. Dedmon, M. M., Lindorff-Larsen, K., Christodoulou, J., Vendruscolo, M. & Dobson, C. M. (2005). Mapping long-range interactions in alpha-synuclein using spin-label NMR and ensemble molecular dynamics simulations. *J. Am. Chem. Soc.* **127**, 476–477.
18. Bussell, R., Jr & Eliezer, D. (2001). Residual structure and dynamics in Parkinson's disease-associated mutants of alpha-synuclein. *J. Biol. Chem.* **276**, 45996–56003.
19. Bertoncini, C. W., Fernandez, C. O., Griesinger, C., Jovin, T. M. & Zweckstetter, M. (2005). Familial mutants of alpha-synuclein with increased neurotoxicity have a destabilized conformation. *J. Biol. Chem.* **280**, 30649–30652.
20. Wilkins, D. K., Grimshaw, S. B., Receveur, V., Dobson, C. M., Jones, J. A. & Smith, L. J. (1999). Hydrodynamic radii of native and denatured proteins measured by pulse field gradient NMR techniques. *Biochemistry*, **38**, 16424–16431.
21. Tanford, C. (1968). Protein denaturation. *Adv. Protein Chem.* **23**, 121–282.
22. Tanford, C. (1961). *Physical Chemistry of Macromolecules, Wiley, New York.*
23. Ikura, M., Kay, L. E. & Bax, A. (1990). A novel-approach for sequential assignment of H-1, C-13, And N-15 spectra of larger proteins-heteronuclear triple-resonance 3-dimensional NMR-spectroscopy–application to calmodulin. *Biochemistry*, **29**, 4659–4667.
24. Eliezer, D., Kutluay, E., Bussell, R., Jr & Browne, G. (2001). Conformational properties of alpha-synuclein in its free and lipid-associated states. *J. Mol. Biol.* **307**, 1061–1073.
25. Panchal, S. C., Bhavesh, N. S. & Hosur, R. V. (2001). Improved 3D triple resonance experiments, HNN and HN(C)N, for HN and ^{15}N sequential correlations in (^{13}C, ^{15}N) labeled proteins: application to unfolded proteins. *J. Biomol. NMR*, **20**, 135–147.
26. McNulty, B. C., Tripathy, A., Young, G. B., Charlton, L. M., Orans, J. & Pielak, G. J. (2006). Temperature-induced reversible conformational change in the first 100 residues of alpha-synuclein. *Protein Sci.* **15**, 602–608.
27. Wishart, D. S., Bigam, C. G., Holm, A., Hodges, R. S. & Sykes, B. D. (1995). ^{1}H, ^{13}C and ^{15}N random coil NMR chemical shifts of the common amino acids. I. Investigations of nearest-neighbor effects. *J. Biomol. NMR*, **5**, 67–81.
28. McCarney, E. R., Kohn, J. E. & Plaxco, K. W. (2005). Is there or isn't there? The case for (and against) residual structure in chemically denatured proteins. *Crit. Rev. Biochem. Mol. Biol.* **40**, 181–189.

29. Serrano, L. (1995). Comparison between the phi distribution of the amino acids in the protein database and NMR data indicates that amino acids have various phi propensities in the random coil conformation. *J. Mol. Biol.* **254**, 322–333.
30. Smith, L. J., Bolin, K. A., Schwalbe, H., MacArthur, M. W., Thornton, J. M. & Dobson, C. M. (1996). Analysis of main chain torsion angles in proteins: prediction of NMR coupling constants for native and random coil conformations. *J. Mol. Biol.* **255**, 494–506.
31. Marsh, J. A., Singh, V. K., Jia, Z. & Forman-Kay, J. D. (2006). Sensitivity of secondary structure propensities to sequence differences between alpha- and gamma-synuclein: implications for fibrillation. *Protein Sci.* **15**, 2795–2804.
32. Lam, S. L. & Hsu, V. L. (2003). NMR identification of left-handed polyproline type II helices. *Biopolymers*, **69**, 270–281.
33. Uversky, V. N., Li, J. & Fink, A. L. (2001). Evidence for a partially folded intermediate in alpha-synuclein fibril formation. *J. Biol. Chem.* **276**, 10737–10744.
34. Bax, A. (2003). Weak alignment offers new NMR opportunities to study protein structure and dynamics. *Protein Sci.* **12**, 1–16.
35. Shortle, D. & Ackerman, M. S. (2001). Persistence of native-like topology in adenatured protein in 8(M urea. *Science*, **293**, 487–489.
36. Mohana-Borges, R., Goto, N. K., Kroon, G. J. A., Dyson, H. J. & Wright, P. E. (2004). Structural characterization of unfolded states of apomyoglobin using residual dipolar couplings. *J. Mol. Biol.* **340**, 1131–1142.
37. Fieber, W., Kristjansdottir, S. & Poulsen, F. M. (2004). Short-range, long-range and transition state interactions in the denatured state of ACBP from residual dipolar couplings. *J. Mol. Biol.* **339**, 1191–1199.
38. Louhivuori, M., Pääkkönen, K., Fredriksson, K., Permi, P., Lounila, J. & Annila, A. (2003). On the origin of residual dipolar couplings from denatured proteins. *J. Am. Chem. Soc.* **125**, 15647–15650.
39. Fredriksson, K., Louhivuori, M., Permi, P. & Annila, A. (2004). On the interpretation of residual dipolar couplings as reporters of molecular dynamics. *J. Am. Chem. Soc.* **126**, 12646–12650.
40. Skora, L., Cho, M. K., Kim, H. Y., Becker, S., Fernandez, C. O., Blackledge, M. & Zweckstetter, M. (2006). Charge-induced molecular alignment of intrinsically disordered proteins. *Angew Chem. Int. Ed. Engl.* **45**, 7012–7015.
41. Cho, M. K., Kim, H. Y., Bernado, P., Fernandez, C. O., Blackledge, M. & Zweckstetter, M. (2007). Amino acid bulkiness defines the local conformations and dynamics of natively unfolded alpha-synuclein and Tau. *J. Am. Chem. Soc.* **129**, 3032–3033.
42. Mittermaier, A. & Kay, L. E. (2006). New tools provide new insights in NMR studies of protein dynamics. *Science*, **312**, 224–228.
43. Shojania, S. & O'Neil, J. D. (2006). HIV-1 Tat is a natively unfolded protein: the solution conformation and dynamics of reduced HIV-1 Tat-(1-72) by NMR spectroscopy. *J. Biol. Chem.* **281**, 8347–8356.
44. Thapar, R., Mueller, G. A. & Marzluff, W. F. (2004). The N-terminal domain of the *Drosophila* histone mRNA binding protein, SLBP, is intrinsically disordered with nascent helical structure. *Biochemistry*, **43**, 9390–9400.
45. Wirmer, J., Berk, H., Ugolini, R., Redfield, C. & Schwalbe, H. (2006). Characterization of the unfolded state of bovine alpha-lactalbumin and comparison with unfolded states of homologous proteins. *Protein Sci.* **15**, 1397–1407.
46. Sung, Y. H. & Eliezer, D. (2006). Secondary structure and dynamics of micelle bound beta- and gamma-synuclein. *Protein Sci.* **15**, 1162–1174.
47. Bouvignies, G., Bernado, P., Meier, S., Cho, K., Grzesiek, S., Bruschweiler, R. & Blackledge, M. (2005). Identification of slow correlated motions in proteins using residual dipolar and hydrogen-bond scalar couplings. *Proc. Natl Acad. Sci. USA*, **102**, 13885–13890.
48. Lakomek, N. A., Carlomagno, T., Becker, S., Griesinger, C. & Meiler, J. (2006). A thorough dynamic interpretation of residual dipolar couplings in ubiquitin. *J. Biomol. NMR*, **34**, 101–115.
49. Syme, C. D., Blanch, E. W., Holt, C., Jakes, R., Goedert, M., Hecht, L. & Barron, L. D. (2002). A Raman optical activity study of rheomorphism in caseins, synucleins and tau. New insight into the structure and behaviour of natively unfolded proteins. *Eur. J. Biochem.* **269**, 148–156.
50. Rath, A., Davidson, A. R. & Deber, C. M. (2005). The structure of "unstructured" regions in peptides and proteins: role of the polyproline II helix in protein folding and recognition. *Biopolymers*, **80**, 179–185.
51. Rucker, A. L., Pager, C. T., Campbell, M. N., Qualls, J. E. & Creamer, T. P. (2003). Host-guest scale of left-handed polyproline II helix formation. *Proteins: Struct. Funct. Genet.* **53**, 68–75.
52. Shi, Z., Woody, R. W. & Kallenbach, N. R. (2002). Is polyproline II a major backbone conformation in unfolded proteins? *Adv. Protein Chem.* **62**, 163–240.
53. Shi, Z., Chen, K., Liu, Z., Ng, A., Bracken, W. C. & Kallenbach, N. R. (2005). Polyproline II propensities from GGXGG peptides reveal an anticorrelation with beta-sheet scales. *Proc. Natl Acad. Sci. USA*, **102**, 17964–17968.
54. Makowska, J., Rodziewicz-Motowidlo, S., Baginska, K., Vila, J. A., Liwo, A., Chmurzynski, L. & Scheraga, H. A. (2006). Polyproline II conformation is one of many local conformational states and is not an overall conformation of unfolded peptides and proteins. *Proc. Natl Acad. Sci. USA*, **103**, 1744–1749.
55. Vucetic, S., Obradovic, Z., Vacic, V., Radivojac, P., Peng, K., Iakoucheva, L. M. *et al.* (2005). DisProt: a database of protein disorder. *Bioinformatics*, **21**, 137–140.
56. Prilusky, J., Felder, C. E., Zeev-Ben-Mordehai, T., Rydberg, E. H., Man, O., Beckmann, J. S. *et al.* (2005). FoldIndex: a simple tool to predict whether a given protein sequence is intrinsically unfolded. *Bioinformatics*, **21**, 3435–3438.
57. McPherson, P. S. (1999). Regulatory role of SH3 domain-mediated protein-protein interactions in synaptic vesicle endocytosis. *Cell Signal*, **11**, 229–238.
58. Kay, B. K., Williamson, M. P. & Sudol, M. (2000). The importance of being proline: the interaction of proline-rich motifs in signaling proteins with their cognate domains. *FASEB J.* **14**, 231–241.
59. Ohtake, H., Limprasert, P., Fan, Y., Onodera, O., Kakita, A., Takahashi, H. *et al.* (2004). Beta-synuclein gene alterations in dementia with Lewy bodies. *Neurology*, **63**, 805–811.
60. Danielsson, J., Jarvet, J., Damberg, P. & Graslund, A. (2005). The Alzheimer beta-peptide shows temperature-dependent transitions between left-handed 3-helix, beta-strand and random coil secondary structures. *FEBS J.* **272**, 3938–3949.
61. Blanch, E. W., Morozova-Roche, L. A., Cochran, D. A., Doig, A. J., Hecht, L. & Barron, L. D. (2000). Is

polyproline II helix the killer conformation? A Raman optical activity study of the amyloidogenic prefibrillar intermediate of human lysozyme. *J. Mol. Biol.* **301**, 553–563.
62. Chellgren, B. W., Miller, A. F. & Creamer, T. P. (2006). Evidence for polyproline II helical structure in short polyglutamine tracts. *J. Mol. Biol.* **361**, 362–371.
63. Bielska, A. A. & Zondlo, N. J. (2006). Hyperphosphorylation of tau induces local polyproline II helix. *Biochemistry*, **45**, 5527–5537.
64. Bhattacharyya, A., Thakur, A. K., Chellgren, V. M., Thiagarajan, G., Williams, A. D., Chellgren, B. W. *et al.* (2006). Oligoproline effects on polyglutamine conformation and aggregation. *J. Mol.Biol.* **355**, 524–535.
65. Hoyer, W., Antony, T., Cherny, D., Heim, G., Jovin, T. M. & Subramaniam, V. (2002). Dependence of alpha-synuclein aggregate morphology on solution conditions. *J. Mol. Biol.* **322**, 383–393.
66. Hansen, M. R., Mueller, L. & Pardi, A. (1998). Tunable alignment of macromolecules by filamentous phage yields dipolar coupling interactions. *Nature Struct. Biol.* **5**, 1065–1074.
67. Rückert, M. & Otting, G. (2000). Alignment of biological macromolecules in novel nonionic liquid crystalline media for NMR experiments. *J. Am. Chem. Soc.* **122**, 7793–7797.
68. Jones, J. A., Wilkins, D. K., Smith, L. J. & Dobson, C. M. (1997). Characterisation of protein unfolding by NMR diffusion measurements. *J. Biomol. NMR*, **10**, 199–203.
69. Farrow, N. A., Zhang, O. W., Szabo, A., Torchia, D. A. & Kay, L. E. (1995). Spectral density-function mapping using 15N relaxation data exclusively. *J. Biomol. NMR*, **6**, 153–162.
70. Ottiger, M., Delaglio, F. & Bax, A. (1998). Measurement of J and dipolar couplings from simplified two-dimensional NMR spectra. *J. Magn. Reson.* **131**, 373–378.
71. Delaglio, F., Grzesiek, S., Vuister, G. W., Zhu, G., Pfeifer, J. & Bax, A. (1995). NMRPipe: a multidimensional spectral processing system based on UNIX pipes. *J. Biomol. NMR*, **6**, 277–293.

Edited by P. Wright

(Received 30 May 2007; received in revised form 7 July 2007; accepted 9 July 2007)
Available online 17 July 2007